Vol 18 No 6, June 2009
1674-1056/2009/18(06)/2377-06

Chinese Physics B

© 2009 Chin. Phys. Soc.
and IOP Publishing Ltd

Transmission spectra through a photonic double quantum well system*

Fei Hong-Ming(费宏明)[a)†], Jiang Yuan-Kai(姜缘开)[b)‡],
Liang Jiu-Qing(梁九卿)[a)], and Lin Duo-Liang(林多樑)[b)]

[a)] *Institute of Theoretical Physics and Department of Physics, Shanxi University, Taiyuan* 030006, *China*

[b)] *Department of Physics, State University of New York at Buffalo, Buffalo, New York* 14260-1500, *USA*

(Received 23 November 2008; revised manuscript received 1 January 2009)

By means of the modal expansion method with an R-matrix propagation algorithm, effects of the coupling between resonance photonic states on the resonance tunneling through a double quantum well structure are investigated. We examine the effects on the transmission spectra due to variation of the second well width and middle barrier thickness. Drastic change of the tunneling spectra is found and analyzed when the wells are filled with left-hand media.

Keywords: double quantum well, R-matrix, left-hand media
PACC: 4270Q, 5225F, 3280

1. Introduction

Photonic band gap (PBG) materials or photonic crystals (PC) have received increasing attention due to their fundamental physics in inhibition of spontaneous emission of light, localization of light as well as their potential applications.[1,2] Photonic material devices may find their applications in optical diodes, optical switches, filters, dielectric reflectors, microwave antennae substrate, photonic crystal lasers, photonic crystal circuits and waveguides.

A complete analogy can be drawn between photonic crystal studies and semiconductor physics.[3] Electronic states are known to exhibit forbidden band gaps in semiconductors. It is found that photonic band gaps exist in which electromagnetic waves cannot propagate. Electronic quantum well systems have been a very active field of research in semiconductor physics up to the present day. It is therefore a natural extension of the analogy to consider the photonic quantum well in a similar fashion. The first theoretical study of a photonic quantum well was reported a few years ago where the resonant tunneling effect was observed in a single well system,[4,5] in which experimental investigation of a photonic quantum well system was first suggested. The fabrication of a photonic quantum well system has been realized and the transmission spectra are observed experimentally.[6] Millimeter size Si_3N_4 spheres are used in this experiment for the construction of photonic crystal slabs which serve as barriers with an air slab between them. The transmission spectra and the intensity of the electric field in the air well of the photonic quantum well are measured by means of a network analyzer (Wiltron 360B). Numerous sharp peaks are observed and the experimental results are found to be consistent with the prediction in [4].

The electronic single and double quantum well systems were initially proposed in early 1960s.[7,8] The electronic double quantum well resonant interband tunneling diodes were predicted in theory and demonstrated in experiments.[9,10] It is shown that the electronic double well system can be far more superior to single well systems in terms of device performance such as the peak current, peak-to-valley ratio, etc. The present paper is a natural extension of our previous work on the single quantum well system.[4] The modal expansion method with an R-matrix propagation algorithm is found to be inherently suitable for photonic crystals of finite thickness. It is less demanding on the computation resources[11,12] and is therefore very effective in the numerical study of transmission spectra of a single well system.[4] Due to difficulties in the fabrication of three-dimensional pho-

*Project supported by the National Natural Science Foundation of China (Grant No 10775091).
†Corresponding author. E-mail: feihm187491@126.com
‡Present address: CodeRyte, Inc., 7500 Old Georgetown Rd., Suite 800, Bethesda, MD 2081

tonic crystals in the optical frequency, the experimental research in photonic crystals is usually carried out for two-dimensional (2D) photonic crystals in the microwave or millimeter wave region because of easy fabrication of (2D) photonic crystals. These experiments in 2D photonic crystals have prompted interest in the theoretical investigation of a 2D system. In this paper, we study the transmission of light through double quantum well structures involving 2D photonic crystal slabs.

2. Method of calculation

We consider a photonic double quantum well system consisting of three thin slabs of 2D photonic crystal with uniform optical medium between the first and second slabs and between the second and third slabs. The photonic crystal slab is an array of infinitely long dielectric cylinders with constant permittivity ϵ. We have calculated the band gap for photonic slabs consisting of dielectric cylinders with a circular cross-section and compared the gap with that for dielectric cylinders with a square cross-section. A comparison of the two cases shows that the band gaps are similar for square and circular cross-sections, but the computing time for a square cross-section is much less. Therefore, we use square cross-section cylinders for the three photonic slabs in the present calculation. The cross-sections of the cylinders are assumed to be a square of side length a. The spatial period of the array of cylinders is d. Figure 1(a) shows the geometry. The crystal is infinitely periodic in the x direction and the cylinders are placed along the y direction. The first, second and third photonic crystal slabs are marked by B1, B2 and B3, with thickness $b1$, $b2$ and $b3$, respectively. The first uniform dielectric region is denoted by W1 with width $w1$, the second is denoted by W2 with width $w2$.

If a photon of frequency ω within the forbidden gap of the 2D photonic crystal slab falls on the surface, the slab of the photonic crystal acts as a potential barrier. Physically, the double quantum well system is shown in figure 1(b), in which the height of the barrier is taken to be the band gap.

The following notation is introduced in the formalism of modal expansion with R-matrix algorithm.

$$\widetilde{E}(x,z)=\begin{bmatrix}E_x(X,z)\\E_y(X,z)\end{bmatrix},$$

$$\widetilde{H}(x,z)=\begin{bmatrix}H_x(X,z)\\H_y(X,z)\end{bmatrix}. \tag{1}$$

The R-matrix is defined by

$$\begin{bmatrix}\widetilde{E}(X,z_1)\\\widetilde{E}(X,z_2)\end{bmatrix}=R(z_2-z_1)\begin{bmatrix}\widetilde{H}(X,z_1)\\\widetilde{H}(X,z_2)\end{bmatrix}. \tag{2}$$

In equation (2) $R(z_2-z_1)$ relates the electric field to the corresponding magnetic field at the sub-layer boundaries. Each spatial period along the z-direction is divided into two sub-layers. For a sub-layer where ϵ is a function of x alone, the details of evaluation of $R(z_2-z_1)$ can be found in [4]. Repeating the above procedure, we can evaluate the R-matrix for the whole slab of the photonic barrier. The R-matrices R^{b1}, R^{b2}, and R^{b3} for the first, second and third photonic slab can now be calculated. The uniform medium or the well is treated as a special case of the photonic crystal with $\epsilon(r)=$ constant. The R-matrix R^{w1}, R^{w2} for the first and second uniform regions can be calculated. The R-matrix for the first quantum well system, can be calculated from the following recursion formula

$$\begin{aligned}
R_{11}^{b1w1b2}&=R_{11}^{b1}+R_{12}^{b1}\left(R_{11}^{w1}-R_{22}^{b1}\right)^{-1}R_{21}^{b1}-R_{12}^{b1}\left(R_{11}^{w1}-R_{22}^{b1}\right)^{-1}R_{12}^{w1}\\
&\quad\times\left[R_{11}^{b2}-R_{22}^{w1}+R_{21}^{w1}\left(R_{11}^{w1}-R_{22}^{b1}\right)^{-1}R_{12}^{w1}\right]^{-1}R_{21}^{w1}\left(R_{11}^{w1}-R_{22}^{b1}\right)^{-1}R_{21}^{b1},\\
R_{12}^{b1w1b2}&=-R_{12}^{b1}\left(R_{11}^{w1}-R_{22}^{b1}\right)^{-1}R_{12}^{w1}\left[R_{11}^{b2}-R_{22}^{w1}+R_{21}^{w1}\left(R_{11}^{w1}-R_{22}^{b1}\right)^{-1}R_{12}^{w1}\right]^{-1}R_{12}^{b2},\\
R_{21}^{b1w1b2}&=R_{21}^{b2}\left[R_{11}^{b2}-R_{22}^{w1}+R_{21}^{w1}\left(R_{11}^{w1}-R_{22}^{b1}\right)^{-1}R_{12}^{w1}\right]^{-1}R_{21}^{w1}\left(R_{11}^{w1}-R_{22}^{b1}\right)^{-1}R_{21}^{b1},\\
R_{22}^{b1w1b2}&=R_{22}^{b2}-R_{21}^{b2}\left[R_{11}^{b2}-R_{22}^{w1}+R_{21}^{w1}\left(R_{11}^{w1}-R_{22}^{b1}\right)^{-1}R_{12}^{w1}\right]^{-1}R_{12}^{b2}.
\end{aligned} \tag{3}$$

The R-matrix for the double well system, $R^{b1w1b2w2b3}$, can be calculated from the following recursion formula

$$
\begin{aligned}
R_{11}^{b1w1b2w2b3} &= R_{11}^{b1w1b2} + R_{12}^{b1w1b2}\left(R_{11}^{w2} - R_{22}^{b1w1b2}\right)^{-1} R_{21}^{b1w1b2} - R_{12}^{b1w1b2}\left(R_{11}^{w2} - R_{22}^{b1w1b2}\right)^{-1} R_{12}^{w2} \\
&\quad \times \left[R_{11}^{b3} - R_{22}^{w2} + R_{21}^{w2}\left(R_{11}^{w2} - R_{22}^{b1w1b2}\right)^{-1} R_{12}^{w2}\right]^{-1} R_{21}^{w2}\left(R_{11}^{w2} - R_{22}^{b1w1b2}\right)^{-1} R_{21}^{b1w1b2}, \\
R_{12}^{b1w1b2w2b3} &= -R_{12}^{b1}\left(R_{11}^{w2} - R_{22}^{b1w1b2}\right)^{-1} R_{12}^{w2}\left[R_{11}^{b3} - R_{22}^{w2} + R_{21}^{w2}\left(R_{11}^{w2} - R_{22}^{b1w1b2}\right)^{-1} R_{12}^{w2}\right]^{-1} R_{12}^{b3}, \\
R_{21}^{b1w1b2w2b3} &= R_{21}^{b3}\left[R_{11}^{b3} - R_{22}^{w2} + R_{21}^{w2}\left(R_{11}^{w2} - R_{22}^{b1w1b2}\right)^{-1} R_{12}^{w2}\right]^{-1} R_{21}^{w2}\left(R_{11}^{w2} - R_{22}^{b1w1b2}\right)^{-1} R_{21}^{b1w1b2}, \\
R_{22}^{b1w1b2w2b3} &= R_{22}^{b3} - R_{21}^{b3}\left[R_{11}^{b3} - R_{22}^{w2} + R_{21}^{w2}\left(R_{11}^{w2} - R_{22}^{b1w1b2}\right)^{-1} R_{12}^{w2}\right]^{-1} R_{12}^{b3}.
\end{aligned} \tag{4}
$$

On the left-hand side of the photonic QW, the electromagnetic field is a superstition of incident wave and reflected wave, while on the right-hand side there is only the transmitted wave. Applying equation (4) to the whole QW system, we find

$$
\begin{bmatrix} \widetilde{E}^t(X) \\ \widetilde{E}^r(X) + \widetilde{E}^{\mathrm{inc}}(X) \end{bmatrix} = R^{b1w1b2w2b3} \begin{bmatrix} \widetilde{H}^t(X) \\ \widetilde{H}^r(X) + \widetilde{H}^{\mathrm{inc}}(X) \end{bmatrix}, \tag{5}
$$

where $\widetilde{E}^{\mathrm{inc}}(X)$, $\widetilde{H}^{\mathrm{inc}}(X)$; $\widetilde{E}^r(X)$, $\widetilde{H}^r(X)$; and $\widetilde{E}^t(X)$, $\widetilde{H}^t(X)$ are incident, reflected and transmitted fields, respectively.

To find the relation between the electric and magnetic fields in the real space, we first Fourier transform them into the momentum space, where they have simple relations, and then transform electric and magnetic fields back from the momentum space. The relation between electric and magnetic fields is then substituted into equation (5) to obtain finally

$$
\begin{bmatrix} R_{11}^{b1w1b2w2b3}\overline{T}_+ - I & R_{12}^{b1w1b2w2b3}\overline{T}_- \\ R_{21}^{b1w1b2w2b3}\overline{T}_+ & R_{22}^{b1w1b2w2b3}\overline{T}_- - I \end{bmatrix} \begin{bmatrix} \widetilde{E}^t(X) \\ \widetilde{E}^r(X) \end{bmatrix} = \begin{bmatrix} -R_{12}^{b1w1b2w2b3}\overline{T}_+\widetilde{E}^{\mathrm{inc}}(X) \\ \left(I - R_{22}^{b1w1b2w2b3}\overline{T}_+\right)\widetilde{E}^{\mathrm{inc}}(X) \end{bmatrix}, \tag{6}
$$

where the matrices employed are defined as follows:

$$
\begin{aligned}
\overline{T}_+ &= F(X,K)\, T_+ F^{-1}(X,K), \\
\overline{T}_- &= F(X,K)\, T_- F^{-1}(X,K)
\end{aligned} \tag{7}
$$

with

$$
T_+ = \begin{bmatrix} 0 & -I \\ I & 0 \end{bmatrix}, \quad T_- = \begin{bmatrix} 0 & I \\ -I & 0 \end{bmatrix}. \tag{8}
$$

It is noted that $F(X,K)$ is a Fourier-transformation matrix defined by $\widetilde{E}(X) = F(X,K)\,\widetilde{E}(K)$ or $\widetilde{H}(X) = F(X,K)\,\widetilde{H}(K)$. In equations (6) and (8), I is the unit matrix. From (6), the transmission spectra through the double photonic quantum well can be calculated.

3. Results and discussion

In the numerical calculations, we choose parameters for the 2D photonic crystal similar to those in the experimental measurement.[13] The cylinders of the photonic crystal are made of aluminum ceramics with a dielectric constant 8.9. The lattice constant is taken to be 1.87 mm, and the side of square cross-section of the cylinder is 0.74 mm. For the uniform medium in the well we assume the vacuum for simplicity. If the electric field is polarized parallel to the rod axis, both our calculation and experimental measurement[13] show that the photonic band gap is between 45 and 70 GHz for a photonic barrier of seven layers of aluminum ceramic rods.

We study in this paper the photonic transport properties of double quantum well systems. The effects of the width variation of the second well and middle barrier on the transmission probability through a double quantum well system are investigated. As is indicated in reference [4], the photonic gap is between 35 and 70 GHz. Therefore, in all calculations of the double quantum well structures that follow, we vary the light frequency within the range from 30 GHz to 80 GHz inside the band gap.

The physical arrangement and the energy dia-

gram of the double quantum-well/triple barrier system are shown in figures 1(a) and 1(b). From the left to right, we denote the barriers by B1, B2 and B3, and their thickness by $b1$, $b2$ and $b3$ respectively. The first quantum wells are denoted by W1 and W2 and their width $w1$ and $w2$.

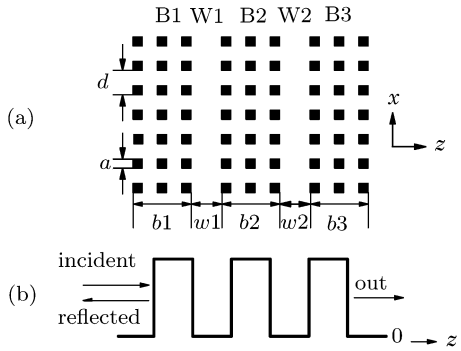


Fig.1. The photonic double quantum well structure. (a) Schematic diagram of the cross-sectional view for the physical arrangement. (b) Double quantum well system as seen by the incident photons with frequency within the band gap.

First, we vary the width of the second well, which leads to an asymmetrical double quantum well structure. The transmission probability is plotted as a function of the incident light frequency in figures 2(a)–2(f) with the second well width $w2$ equal to 6, 7, 8, 9, 10, and 11 mm respectively. All other dimensions of the system are kept as constant. All three barriers have three layers of unit cells in the z-direction. $b1 = b2 = b3 = 5.61$ mm, $w1 = 9$ mm. From figures 2(a)–2(f), we see that resonance tunneling occurs at certain frequencies. The peaks are identified by P_{ij} where $i = 1$, 2 indicates the first or the second well and j indicates the relative order of the resonance frequency. By comparing the peak frequencies with that of figure 3(b) in reference [4], we observe that the position of the resonance frequency in the first well, P_{11}, P_{12} and P_{13}, do not change, while the resonance frequency in the second well is shifting to the left and the spacing between them is decreasing at the same time. This can be explained by the fact that the resonance frequency is given by $f_n = nc/w$, and is inversely proportional to the well width. When $w1$ and $w2$ are not equal, the transmission probability is around 0.2, indicating that the resonant states inside the two wells have very weak interactions and are thus almost independent of each other in most cases. Under these circumstances, the photonic states in each well are basically localized within the quantum well. From figure 2(a) to 2(f), the resonance peak of the second well is shifting toward the left. Sometimes it may come close to the resonance in the first well, implying the strong coupling between the two wells, and the resonance peaks become higher. The situation is illustrated by P_{21} and P_{11} in Fig.2(a), P_{23} and P_{13} in figure 2(b), P_{25} and P_{12} in figure 2(f). The perfect transmission is observed when the double quantum well is symmetric with $w1 = w2 = 9$ mm as shown in figure 2(d). The resonance frequency for the first quantum well overlaps with that of the second. It is seen that a resonance peak in the single well case reference [4] as in figure 3(b) splits now into two sharp spectral lines. In other words, the resonance energies in double quantum well split into doublets. In this case, coupling between the two wells is strongest and photonic states are extended to the two wells. It is interesting to note that both theoretical and experimental research of electronic double quantum well systems observed similar double resonance effects.[10,14,15]

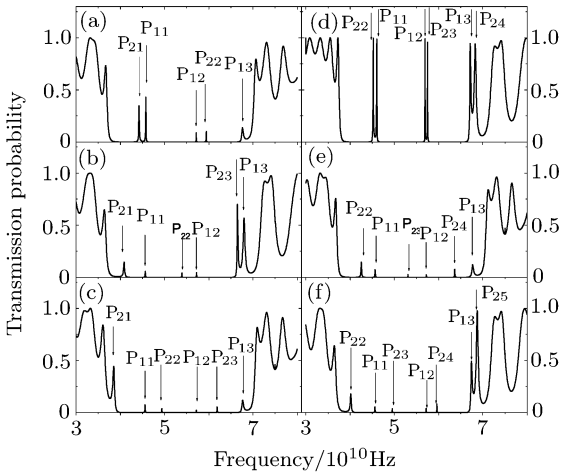


Fig.2. Transmission probability versus the incident light frequency for a double quantum well and triple barrier system with the second well width (a) $w2 = 6$ mm, (b) $w2 = 7$ mm, (c) $w2 = 8$ mm, (d) $w2 = 9$ mm, (e) $w2 = 10$ mm, (f) $w2 = 11$ mm.

Next we consider a symmetric double quantum well structure and vary the barrier width. The transmission probability versus the incident light frequency is depicted in figures 3(a)–3(d) with the middle barrier consisting of 2, 4, 6 and 9 layers of unit cells in z direction, respectively. All other dimensions of the double well are kept constant. They are $w1 = w2 = 9$ mm, $b1 = b3 = 5.61$ mm. It is found that the separation between the double peaks is decreasing as the number of layers of crystal for the middle barrier increases from 2 to 6 layers. For the case of a 2-layer barrier in figure 3(a), the splitting is most evident and the separation

between the doublets is the biggest. This indicates the strongest coupling between resonant states of the two wells. As the middle barrier becomes wider, the coupling is weaker. When the middle barrier is increased to 9 layers of crystal, interaction between the two wells almost vanishes and the perfect transmission disappears.

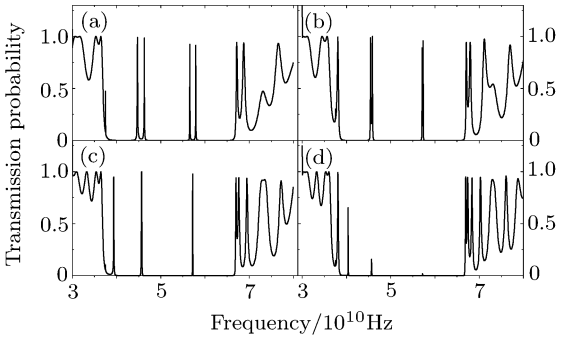


Fig.3. Transmission probability versus the incident light frequency for a double quantum well and triple barrier system with the middle barrier consisting of the crystal (a) 2 layers, (b) 4 layers, (c) 6 layers, (d) 9 layers.

So far we have considered systems with quantum wells left empty between photonic barriers. We now turn our attention to the effects of various well media. It is well known that light propagates at a reduced speed in media characterized by the permittivity. The resonance frequency is proportional to the light speed and inversely proportional to the well width, namely, $f_n = nv/w$, where n is the integer and v stands for the light speed. Hence the resonance frequency as well as the virtual state energy in the well decreases with the increasing permittivity of the well medium. The situation is depicted in figure 4 where the transmission rate variation as a function of the incident

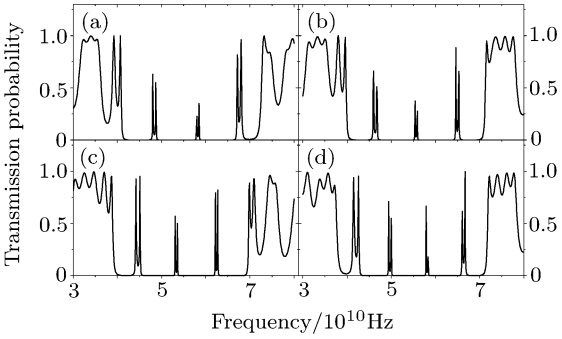


Fig.4. Transmission probability versus the incident light frequency for a double quantum well and triple barrier system with the two wells consisting of medium with (a) $\epsilon = 1.6$, (b) $\epsilon = 1.8$, (c) $\epsilon = 2.0$, (d) $\epsilon = 2.2$.

frequency is illustrated for different permittivities. It is clearly seen that the resonance peak splits into two, and moves toward the low-frequency as the permittivity increases. This confirms the above analysis, the reduced light speed has the same effect as increasing well widths in that both lower the resonance peak frequency.

When the two wells are filled with different media, the resonance transmission spectra are illustrated in figure 5. The asymmetry of the system is due completely to the different media, but the structure remains geometrically symmetric. In the numerical calculation, we take the well width to be 0.9 cm. It is observed from figure 5(a)–5(d) that the level splitting is destroyed, and the resonance frequencies are greatly influenced with level separation increased due to different permittivity.

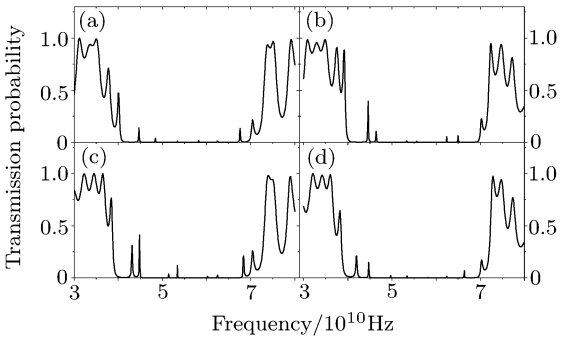


Fig.5. Transmission probability versus the incident light frequency for a double quantum well and triple barrier system with the second well medium with (a) $\epsilon_2 = 1.6$, (b) $\epsilon_2 = 1.8$, (c) $\epsilon_2 = 2.2$, (d) $\epsilon_2 = 2.4$. In all cases the first well medium is $\epsilon_1 = 2.0$.

Most materials familiar to us are right-handed with positive permittivity and permeability. It was suggested that there also exist left-handed (LH) materials which exhibit extraordinary behavior such as the inverse Doppler effect, inverse Snell law, reverse Cerenkov radiation. Here we explore the effect of LH media on the resonance transmission. When both the wells are filled with the same LH medium of permeability $\mu = -1$, the results for various permittivity values are plotted in figures 6(a)–6(d). The well width remains to be 0.9 cm, and the barrier thickness is still three layers of photonic crystal. By comparing figures 6(a), 6(b), 6(c) and figures 4(a), 4(b), 4(d), it is seen that the peak splitting remains perfect. But the spectrum appears to be very different, and the number of peaks is evidently decreasing. This is perhaps because the wave vector and energy flow moves in opposite directions. In other words, the group velocity and phase velocity of the electromagnetic wave are in

opposite directions.

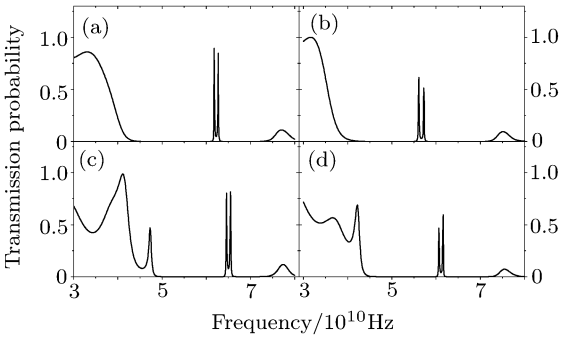


Fig.6. Transmission probability versus the incident light frequency for a double quantum well and triple barrier system with the two wells consisting of medium with (a) $\epsilon = -1.6$, (b) $\epsilon = -1.8$, (c) $\epsilon = -2.2$, (d) $\epsilon = -2.4$.

Finally, we consider the case in which, W1 is filled by RH material and W2 by LH material. The resonance transmission peaks no longer exhibit splitting and the transmission rate is reduced appreciably. Only one peak in figure 7(b) is high and all other peaks are rather low. It is interesting to note that the high transmission occurs at about the same position as those in figures 4(b) and 6(b), indicating the strong coupling of the two media near the resonance frequency. The disappearance of resonant peak-splitting in figure 7 can be understood by the destructive interference due to the opposite propagating direction of the light in LH and RH materials.

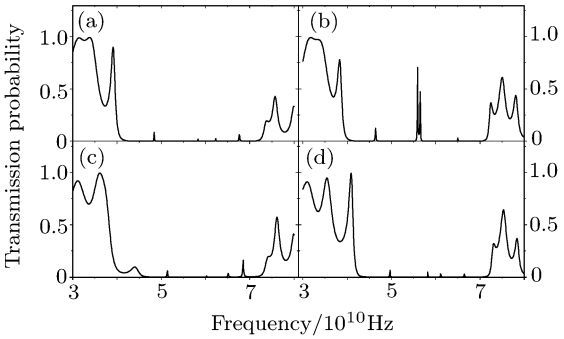


Fig.7. Transmission probability versus the incident light frequency for a double quantum well and triple barrier system with the two wells consisting of medium with (a) $\epsilon_1 = -1.6$, $\epsilon_2 = 1.6$, (b) $\epsilon_1 = -1.8$, $\epsilon_2 = 1.8$, (c) $\epsilon_1 = -2.2$, $\epsilon_2 = 2.2$, (d) $\epsilon_1 = -2.4$, $\epsilon_2 = 2.4$.

4. Conclusion

In summary, we have studied the the transmission spectra of photons through a coupled double-well system showing the typical two-fold splitting of resonance peaks. The resonant frequencies can be controlled by the well width and the coupling strength between the two wells. Such structures are shown to act as the millimeter-wave band-stop and discrete-frequency-pass filters. Of special interest is the disappearance of resonant peak-splitting resulted by the destructive interference in the LH and RH well media. Our theoretical predictions, which may be useful in the practical design of photonic filters, should be observed experimentally.

References

[1] Yablonovitch E 1987 *Phys. Rev. Lett.* **58** 2059
[2] John S 1987 *Phys. Rev. Lett.* **58** 2486
[3] Joannopoulos John D, Meade Robert D and Winn Joshua N 1995 *Photonic Crystals: Molding the Flow of Light* (Princeton: Princeton University Press)
[4] Jiang Y, Niu C and Lin D L 1999 *Phys. Rev.* B **59** 9981
[5] Jiang Y K 2005 *PhD dissertation*, State University of New York at Buffalo, Buffalo, New York
[6] Yano S, Segawa Y, Bae J S, Mizuno K, Miyazaki H, Ohtaka K and Yamaguchi S 2001 *Phys. Rev.* B **63** 153316
[7] Iogansen L V 1991 in *Semiconductor Devices: Pioneering Papers*, ed Sze S M (Singapore: World Scientific) p719
[8] Iogansen L V 1964 *Zh. Eksp. Teor. Fiz.* **47** 270
Iogansen L V 1965 *Sov. Phys. JETP* **20** 180
[9] Sweeny M and Xu J M 1989 *Appl. Phys. Lett.* **54** 546
[10] Day D J, Chung Y, Webb C, Eckstein J N, Sweeny M and Xu J M 1990 *Appl. Phys. Lett.* **57** 1260
[11] Elson J M and Tran P 1995 *J. Opt. Soc. Am.* A **12** 1765
[12] Elson J M and Tran P 1996 *Phys. Rev.* B **54** 1711
[13] Robertson W M, Arjavalingam G A, Meade R D, Brommer K D, Rappe A M and Joannopoulos J D 1992 *Phys. Rev. Lett.* 68 2023
[14] Niu C, Liu L and Lin T 1995 *Phys. Rev.* B **51** 5130
[15] Liu J, Sun J Q, Huang C Q, Chen M and Huang D X 2008 *Chin. Phys.* B **17** 1674